NUREG/CR-4383
SAND85-0012
R7
Printed September 1985

High Pressure Ejection of Melt From a Reactor Pressure Vessel

The Discharge Phase

Marty Pilch, William W. Tarbell

Prepared by
Sandia National Laboratories
Albuquerque, New Mexico 87185 and Livermore, California 94550
for the United States Department of Energy
under Contract DE-AC04-76DP00789

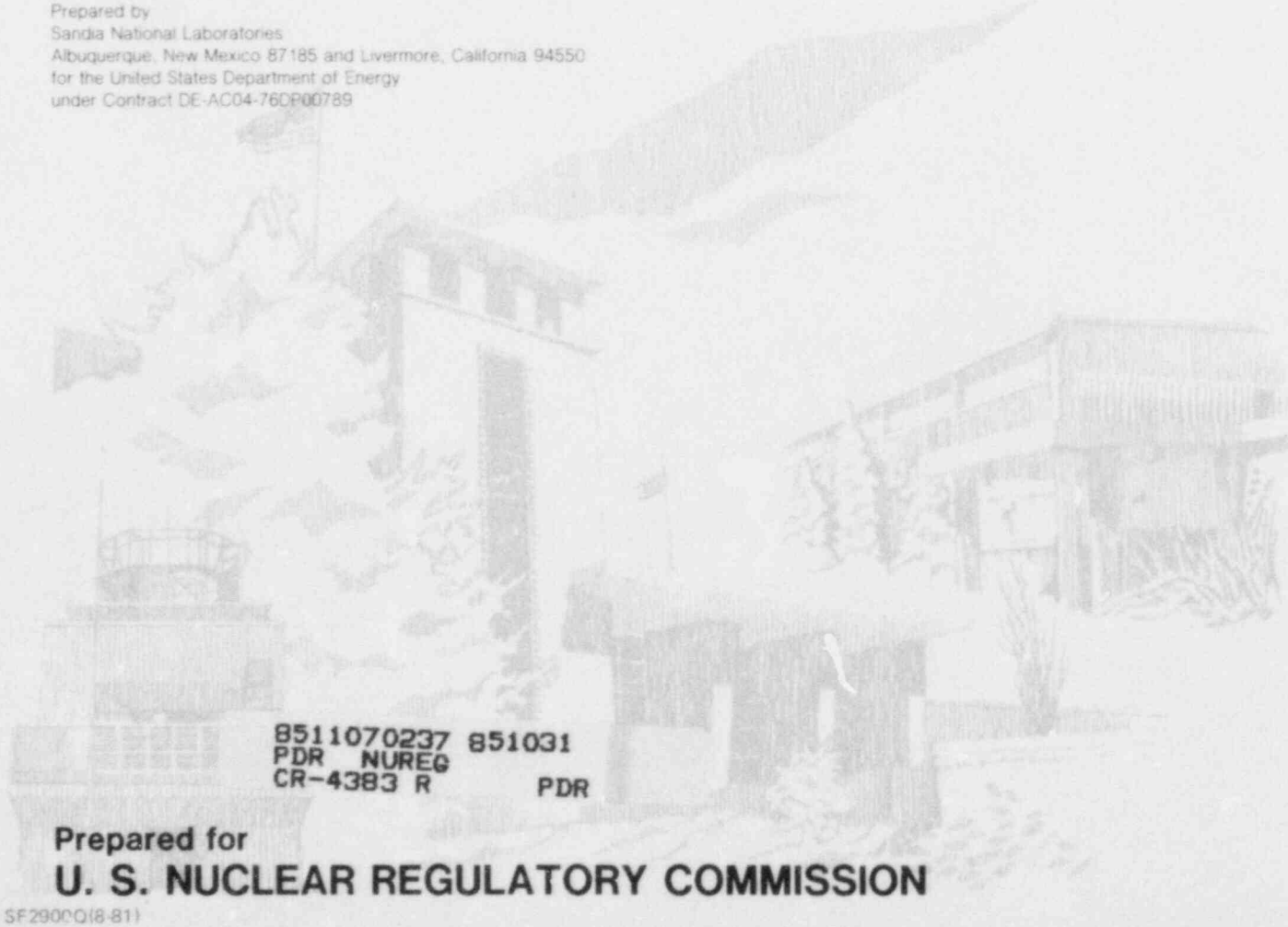

Prepared for
U. S. NUCLEAR REGULATORY COMMISSION

Available from

Superintendent of Documents
U.S. Government Printing Office
Post Office Box 37082
Washington, D.C. 20013-7982

and

National Technical Information Service
Springfield, VA 22161

NUREG/CR-4383
SAND85-0012
R7

HIGH PRESSURE EJECTION OF MELT FROM A REACTOR PRESSURE VESSEL

THE DISCHARGE PHASE

MARTY PILCH
WILLIAM W. TARBELL

September 1985

Sandia National Laboratories
Albuquerque, NM 87185
Operated by
Sandia Corporation
for the
U.S. Department of Energy

Prepared for
Containment Systems Research Branch
Division of Accident Evaluation
Office of Nuclear Regulatory Research
U.S. Nuclear Regulatory Commission
Washington, DC 20555
Under Memorandum of Understanding DOE 40-550-75
NRC FIN A-1218

ABSTRACT

Recent probabilistic risk-assessment studies identified potential accident sequences in which reactor vessel failure occurs while the primary system is at elevated pressure. The phenomenology of the discharge phase is reviewed here. We propose an improved model for hole ablation following vessel failure, and we compare the model with experiment data. Gas blowthrough is identified as a mechanism that allows steam to escape through the vessel breach before melt ejection is complete. Gas blowthrough leads to pneumatic atomization of the remaining melt before significant depressurization of the primary system occurs.

CONTENTS

FIGURES

TABLES

1. INTRODUCTION

Recent probabilistic risk-assessment studies [1,2] identified potential accident sequences in which reactor vessel failure occurs while the primary system is at elevated pressure. These studies argue that melt is forcibly discharged from the pressure vessel, swept from the reactor cavity by blowdown gas, and deposited as a coolable debris bed on the containment floor. Benign termination is not confirmed by recent experiments conducted at Sandia National Laboratories (SNL) [3,4,5]. These experiments confirm that debris is swept from the cavity; however, they also show that highly fragmented debris may be ejected into the containment atmosphere where thermal and chemical energy is liberated rapidly from the debris. Containment pressurization resulting from direct heating of the containment atmosphere by airborne debris might threaten the integrity of the reactor containment. Consequently, a better understanding of mechanisms leading to debris sweepout from the cavity, debris fragmentation, and debris transport into the containment atmosphere is required. This paper discusses recent improvements to our understanding of the discharge phase only; future papers will discuss the sweepout phase and the direct heating phase.

The Zion Probabilistic Safety Study (ZPSS) [1] argues that melt is forcibly driven from the pressure vessel as a coherent jet. Significant ablation of the hole is predicted to occur during melt discharge. Depressurization of the primary system occurs only after <u>all</u> the melt is discharged from the reactor vessel.

Experiments at SNL [3,4,5] show that melt does not exit the pressure vessel as a coherent jet. Instead, the experiments and analysis show that the jet is disrupted outside the hole by the rapid effervescence of dissolved gas in the melt (N_2 in the SNL experiments and H_2 in the reactor accident). The SNL experiments confirm that melt ejection is accompanied by significant ablation of the hole; however, the ZPSS model must be modified in order to predict these experiments.

Gas blowthrough is another process that was not anticipated in the ZPSS analysis. Gas blowthrough, which has been observed during the rapid drainage of fuel tanks, occurs when a funnel-like dip forms on the free surface of the liquid allowing the simultaneous discharge of gas and liquid through the breach in the reactor vessel. This means that depressurization of the primary system begins before all the melt is discharged from the reactor vessel, and this leads to pneumatic atomization of the liquid passing through the hole during the two phase blowdown. Catton [6] has suggested that gas blowthrough allows

depressurization of the primary system to occur before a significant fraction of the melt is ejected from the pressure vessel. Catton argues that the melt remaining in the pressure vessel drains under gravity only after blowdown of the primary system is complete; consequently, a large portion of the melt cannot be swept from the cavity by the blowdown gas.

2. MODEL

The models presented here explicitly couple relevant processes associated with melt discharge from the reactor vessel. These models are scheduled for implementation into MELPROG [7], a large system code that mechanistically tracks the invessel formation of molten core debris, vessel failure, and debris relocation from the reactor cavity. This paper presents results obtained from a fast-running stand-alone code that exploits model simplifications that will not be necessary when the models are placed into MELPROG.

In the following discussion, we assume that the core debris, which accumulates in the lower head of the reactor vessel prior to vessel failure, behaves as a fluid. It is possible that the core debris is a solid/liquid slurry instead of a pure liquid. The processes discussed below are still relevant provided the slurry behaves as a fluid; pneumatic atomization, however, can only occur to the liquid phase of the debris.

2.1 Melt Discharge

The melt mass (M_L) remaining in the reactor vessel is obtained from the continuity equation

$$\frac{dM_L}{dt} = -\dot{M}_L, \tag{1}$$

where $\dot{M}_L$ is the mass flow rate of liquid out the hole.

$$\dot{M}_L = \rho_L A_L V_L \tag{2}$$

Here ρ_L is the average density of the liquid; and V_L is the average velocity of liquid exiting the pressure vessel. Prior to gas blowthrough, A_L is the simply the area of the hole in the

reactor vessel. After gas blowthrough, A_L represents the flow area of liquid out the hole, which is less than the area of the hole; this will be discussed further in the section on gas blowthrough.

The melt velocity (V_L) is obtained from the quasi-steady Bernoulli equation, even after gas blowthrough has occurred.

$$V_L = C_d \left[\frac{\frac{2(P_{ps}-P_c)}{\rho_L} + 2gH}{1 - \left[\frac{A_L}{A_s}\right]^2} \right]^{1/2} \qquad (3)$$

Here C_d is the discharge coefficient; P_s is the instantaneous pressure inside the primary system; P_c is the pressure inside the reactor cavity; g is the acceleration due to gravity, H is the instantaneous depth of the melt inside the reactor vessel; and A_s is the instantaneous area of the free surface of the melt pool inside the pressure vessel.

2.2 Hole Ablation

The ZPSS analysis concluded that rapid hole ablation begins shortly after the onset of melt discharge through a failed instrument-tube penetration in the reactor vessel. The ablation rate is determined by equating the the convective energy transfer from the the molten fuel to the energy required to heatup and melt the steel.

$$\frac{dD}{dt} = \frac{2h\ \Delta T}{\rho_w[C_{p,w}(T_{m,w}-T_w) + h_{f,w}]} \qquad (4)$$

$$\Delta T = T_f - T_{m,f} \quad \text{ZPSS model} \qquad (5)$$

$$\Delta T = T_f - T_{m,w} \quad \text{Current model} \tag{6}$$

Here D is the instantaneous diameter of the hole in the reactor vessel; T_f is the temperature of the molten fuel; $T_{m,f}$ is the melting temperature of the fuel; $T_{m,w}$ is the melting temperature of the wall (i.e., the wall of the pressure vessel which is steel); h is the heat transfer coefficient from the molten fuel; ρ_w is the density of the pressure vessel; $C_{p,w}$ is the specific heat of the wall; and $h_{f,w}$ is the heat of fusion of the wall.

The ZPSS analysis further concluded that a thin crust (66μm in a supporting calculation) insulated the ablating steel from the molten fuel; consequently, the temperature difference between molten and solidified fuel (Equation 5) governs ablation. According to the ZPSS model, hole ablation will not occur unless the melt is superheated. We feel that such a thin crust is not stable and cannot prevent molten fuel contact with molten steel; therefore, the temperature difference between fuel and molten steel (Equation 6) governs hole ablation.

The small length-to-diameter ratio (L/D) of the ablating hole coupled with rapid ablation dictates careful treatment of the heat transfer coefficient in Equation 4. Development of the thermal and hydrodynamic boundary layers is incomplete (boundary layer thickness less than hole radius) for the small L/D ratio associated with an ablating hole in a reactor vessel. Consequently, the heat transfer coefficient is larger than would be expected for fully developed flow in a long tube. The ZPSS analysis does not consider this entrance region effect. We recommend choosing the larger value of h as determined from a flat plate correlation and from a tube correlation for fully-developed turbulent flow. Our experience, however, is that the flat plate correlation is almost always the appropriate choice for both experiments and reactor analysis.

Flat plate correlation [8]

$$h = 0.0292 \frac{k_L}{L} Re_L^{0.8} Pr^{0.33} \tag{7}$$

Tube correlation [8]

$$h = 0.023 \frac{k_L}{D} Re_d^{0.8} Pr^{0.33} \qquad (8)$$

Here h is the local heat transfer coefficient at the breach exit; k_L is the thermal conductivity of the molten fuel; Re_L is the Reynolds number based on the length (L) of the hole; Re_d is the Reynolds number based the the instantaneous diameter (D) of the hole; and Pr is the Prandtl number of the molten fuel.

Actually, the heat transfer coefficients given by Equations 7-8 are appropriate only for nonablating surfaces. If the ablation rate ($\dot{D}$) is large, then the heat transfer coefficient is reduced because of 'transpiration cooling' of the boundary layer [9]. The modified coefficient is given by

$$h = h \frac{\beta}{e^{\beta} - 1} \qquad (9)$$

where,

$$\beta = \frac{\rho_{mw} C_{p,mw} \dot{D}}{2h} \quad . \qquad (10)$$

Here ρ_{mw} and $C_{p,mw}$ are the density and specific heat of the molten wall material (steel); and $\dot{D}$ is the ablation rate i.e., the rate change of hole diameter.

The effective heat transfer coefficient is significantly reduced when gas blowthrough occurs. Only the molten fuel component of the two phase mixture passing through the hole is capable of ablating the steel; the blowdown gas (steam and hydrogen) is not hot enough (~600 K) to melt the pressure vessel wall. Following gas blowthrough, we reduce the heat transfer coefficient by the relative of amount of molten fuel that is in contact with the steel.

$$h = h \frac{A_L}{A_h} \qquad (11)$$

Here A_h is the area of the hole in the pressure vessel.

Hole ablation has been observed in experiments at SNL where a molten mixture of Fe and Al_2O_3 (T_f=2800 K) was ejected under pressure from a steel pressure vessel (T_w=300 K). Table I compares the observed hole size after complete discharge of melt with model predictions. The model proposed here agrees well with the data. Table II shows the thermophysical propeties used in the calculations.

2.3 Gas Blowthrough

During the process of withdrawing fluids from tanks, surface distortion and subsequent gas ingest has been observed in situations where no liquid rotation have been present [10]. The distortion takes the form of a funnel-like depression of the liquid surface over the outlet hole, which leads to blowthrough of gas in the outlet before all of the liquid has drained from the tank. This phenomena becomes more important as the flow rate out the hole increases.

Consider a very deep pool of liquid draining through a hole. Initially, the free surface of the liquid pool remains level as the pool drains. However, surface distortion and gas blowthrough develop very rapidly when the pool has drained down to some critical depth (H'). Based on experiment measurements of H' in cylindrical and hemispherical tanks, Gluck [10] proposed the following empirical correlation, which we use in our work.

$$H' = 0.43 \left(\frac{4}{\pi} A_s\right)^{0.5} \tanh\left[\left(\frac{A_L}{A_s}\right)^{0.5} Fr^{0.25}\right] \qquad 10^2 < Fr < 10^6 \qquad (12)$$

$$Fr = \frac{V_L^2}{g \left(\frac{4}{\pi} A_L\right)^{1/2}} \qquad \text{Froude number} \qquad (13)$$

Table I

Comparison of Hole Ablation Models With Experiment Data

Test	ΔP(MPa)	d_0(cm)	L(m)	Observed D_f(cm)	Current Model D_f(cm)	ZPSS Model D_f(cm)
HIPS-1J	9.69	2.54	2.54	5.08[a]	5.08	4.78
HIPS-2C	11.7	2.54	2.54	5.5-7	6.40	4.76
HIPS-3J	4.85	2.54	5.08	6-7	6.32	4.87

a) Ablation limited by a graphite shield

Table II

Thermophysical Properties Used in Model Predictions

	Fe/Al_2O_3 Mixture	Core Debris	Steel Vessel
k(W/m/K)	12	11	
$\rho(Kg/m^3)$	3843	8000	7817
$C_p(J/kg/K)$	1086	485	543
$h_f(J/Kg/K)$			2.7e5
μ(Pa-s)	2.9e-3	4.3e-3	
σ(N/m) UO_2		.5	
σ(N/m) Steel		1.5[a]	
T_m(K)	2323	2530	1700

a) Surface tension of steel could be significantly lower depending on O_2 concentration

Careful examination of Equation 12 shows that H' is independent of A_s (for a fixed flow rate) when $A_s/A_L > 400$. The critical depth (H') decreases for smaller values of A_s/A_L; thus, gas blowthrough is delayed in smaller tanks that otherwise have the same hole size and discharge rate.

The expected range of Froude numbers for the SNL experiments and the reactor accident are 10^3 to 10^4, within the applicable range of Gluck's correlation. Keep in mind that prior to gas blowthrough $A_L = A_h$.

Equation 13 says that the critical depth for gas blowthrough (H') is calculated given the liquid flow area ($A_L = A_h$) inside the hole. We reverse the logic following gas blowthrough. Given the instantaneous pool depth (H), we calculate the area of liquid flow (A_L) inside the hole. This ensures that flow rate of liquid out the hole is sufficient to satisfy the condition for gas blowthrough.

$$A_L = A_h \left[\frac{\operatorname{arctanh}\left(\dfrac{H}{0.43 \left(\frac{4}{\pi} A_s\right)^{0.5}} \right)}{\left(\frac{A_h}{A_s}\right)^{0.5} Fr^{0.25}} \right]^{8/3} \qquad (14)$$

$$Fr = \frac{V_L^2}{g \left(\frac{4}{\pi} A_h\right)^{0.5}} \qquad (15)$$

2.4 Blowdown of the Primary System

The ZPSS analysis assumes isothermal blowdown of the primary system.

$$\frac{dP_{ps}}{dt} = - \frac{\dot{M}_g}{M_g} P_{ps} \qquad (16)$$

Here $\dot{M}_g$ is the mass flow rate of blowdown gas from the primary system; and M_g is the gas mass remaining in the primary system, which is determined by a continuity equation.

$$\frac{dM_g}{dt} = -\dot{M}_g \qquad (17)$$

In reality, the blowdown of the primary system is more likely to be isentropic instead of isothermal. Isentropic expansion leads to condensation of the initially saturated steam, which complicates the current analysis. Consequently, we also assume isothermal blowdown in the calculations that follow. We do not feel that the assumption of isothermal blowdown significantly alters the conclusions drawn from the sample calculations.

Two-phase blowdown of the primary system commences at the instant of gas blowthrough. The liquid flow rate is given by Equations 2,3,and 14. Assuming separated flow, the gas flow rate is given by

$$\dot{M}_g = C_d(A_h - A_L)P_{ps}\left[\frac{2}{RT_{ps}}\frac{\gamma}{\gamma-1} r^{2/\gamma}\left[1 - r^{(\gamma-1)/\gamma}\right]\right]^{1/2}, \qquad (18)$$

where

$$r = \left[\frac{2}{\gamma-1}\right]^{\frac{\gamma}{\gamma-1}} \qquad (19)$$

when the flow is choked and

$$r = \frac{P_{ps}}{P_c} \qquad (20)$$

when the flow is not choked. Here C_d is the discharge coefficient; R is the gas constant; T_{ps} is the gas temperature in the primary system; and γ is the isentropic exponent.

2.5 Jet Disruption

Jet disruption during melt discharge occurs by two main processes: effervescing gas and pneumatic atomization. Jet disruption by effervescing gas occurs when hydrogen rapidly comes out of solution with the steel component of molten core debris. Pneumatic atomization occurs following gas blowthrough. Here the relative velocity between gas and liquid in the vessel breach is responsible for liquid atomization. These atomization processes can be sufficiently violent so as to be a potential source of aerosols. In addition, some fraction (i.e., the small particle portion of the particle size distribution) of the atomized debris may be carried directly out of the cavity without ever impacting surfaces of the cavity.

The violent disruption of jets by effervescing gas is a process that has been exploited commercially by the steel industry [11,12,13]. Vacuum degassing of steel melts is a process that removes unwanted nydrogen from molten steel by teaming the melt into a vacuum chamber. The effervescing hydrogen violently fragments the jet into particles of a few hundred microns in size, and the large surface area of the particles allows for the rapid diffusion of the remaining hydrogen from the melt.

This process is quite similar to what can happen in a reactor accident. Powers [14] has shown that hydrogen rapidly goes into solution with the steel component of molten core debris and that the solubility of hydrogen in steel is quite high at the elevated temperatures and pressures that could exist in the primary system prior to vessel failure. The effervescence of hydrogen from the molten core debris will violently fragment the jet when melt is ejected into the low pressure environment in the reactor cavity.

Disruption of thermite jets by the effervescence of nitrogen gas has been observed in experiments at SNL [3,4,5]. The observed jet disruption and aerosol production are indicative of what can happen in the reactor accident because the solubility of N_2 in the iron phase of thermite is similar to the solubility of H_2 in the steel phase of molten core debris.

A mechanistic model does not exist currently that can predict the observed particle sizes produced by effervescing gas. We note, however, that the solubility of H_2 in steel is about a factor of 5 larger in the reactor accident when compared to typical vacuum degassing processes. This suggests that jet disruption might be more energetic in the reactor accident, particularly when molten steel is stratified from the more dense constituents of core debris. On the other hand, molten core debris is less than 20% steel, thus compensating for the higher solubility if the molten steel is well mixed with the remainder of the melt. Extrapolation of observations from vacuum degassing to the reactor accident becomes even more difficult because the jet diameter in the reactor accident could be 10-50 times larger than those commonly used in vacuum degassing. Quantitative predictions or extrapolations cannot be made until a mechanistic model, which is being developed at SNL, becomes available.

Pneumatic atomization occurs when liquid and gas are simultaneously accelerated through an orifice. The liquid is atomized by the gas because of the difference in relative velocities as each phase passes through the orifice. Although pneumatic atomizers have been produced commercially and studied extensively since the early 1900's, there is no universally accepted correlation (or theory) for the observed particle sizes. However, the literature does tell us that the distribution of particle sizes is log-normal with a mass median size (d_m) and a geometric standard deviation (σ_g). We select 3 correlations for comparison from the dozens that appear in the literature. We chose these correlations because they are dimensionless and because each contains the important ratio of gas-to-liquid flow rate.

Deyson correlation [15]

$$\frac{d_m}{d_L} = \frac{8\left[1 + 2.75\left(\frac{\dot{M}_L}{\dot{M}_g}\right)^{0.66}\right]}{\left[\frac{\rho_L}{\rho_g}\frac{d_L}{d_g}\,We\right]^{1/2}} \qquad (21)$$

Lubanska correlation [16]

$$\frac{d_m}{d_L} = 50 \left[\frac{1}{We} \left(\frac{\rho_g}{\rho_L}\right)^2 \frac{\mu_L}{\mu_g} \left(1 + \frac{\dot{M}_L}{\dot{M}_g}\right)\right]^{1/2} \tag{22}$$

Wigg correlation [17]

$$\frac{d_m}{R_g} = 200 \frac{\left(\frac{\rho_g}{\rho_L}\right)^{0.2} On^{0.6} Re^{0.1}}{We'^{0.5}} \left[1 + \frac{\dot{M}_L}{\dot{M}_g}\right]^{1/2} \tag{23}$$

The following definitions apply to the above equations.

$$d_L = \left[\frac{4}{\pi} A_L\right]^{1/2} \tag{24}$$

$$d_g = \left[\frac{4}{\pi} (A_h - A_L)\right]^{1/2} = 2R_g \tag{25}$$

$$We = \frac{\rho_g (V_g - V_L)^2 d_L}{\sigma} \qquad \text{Weber number} \tag{26}$$

$$We' = \frac{\rho_g (V_g - V_L)^2 R_g}{\sigma} \tag{27}$$

$$On = \frac{\mu_L}{[\rho_L \sigma R_g]^{.5}} \qquad \text{Ohnesorge number} \tag{28}$$

$$Re = \frac{\dot{m}_L}{R_g \mu_L} \quad \text{Reynolds number} \tag{29}$$

Here d_L and d_g are the equivalent diameter of the liquid and gas streams in the orifice; R_g, is the gas core radius or the gas annulus thickness; μ_L and μ_g are the viscosities of the liquid and the gas; and σ is the liquid surface tension.

Reported values [16,18,19] of the geometric standard deviation (σ_g) for pneumatic atomization range from 1.4 (i.e., a very narrow distribution) to 10 (i.e., a very broad distribution). Lubanska [16], Hugo [18], and Gretzinger [19] have correlated σ_g with the mass median particle size (d_m expressed in microns). These correlations are not dimensionless. Furthermore, Lubanska and Hugo report conflicting results; Lubanska found that σ_g increases with increasing d_m while Hugo found that σ_g decreased with increasing d_m. We conclude that reasonable estimates of σ_g cannot be made at this time.

Each of the above equations shows a different dependence on length scale and properties of the liquid and gas; consequently, we recommend caution when scaling up from the comparatively small devices on which the correlations are based to the full reactor scale.

3. MODEL RESULTS

We now apply the models developed above to the small break LOCA accident [1] for a large PWR. Here the system pressure is 7 MPa, and the pressure in the reactor cavity is .3 MPa. The volume of the primary system is 340 m^3. The mass of core debris is treated parametrically with a maximum mass of 134 tonnes (whole core). The melt is assumed to contain no superheat at 2530 K. The reactor vessel is initially at 600 K, and the vessel is 0.14 m thick. Thermophysical properties used in the analysis are summarized in Table II.

3.1 Melt Discharge

Figure 1 shows how much mass remains in the reactor vessel as a function of time and initial mass of debris in the lower head for the small break LOCA accident. Mass discharge is complete in 2-4 seconds regardless of the initial mass at the time of vessel failure. This is because the discharge time is dominated by the hole ablation rate. The probability of multiple

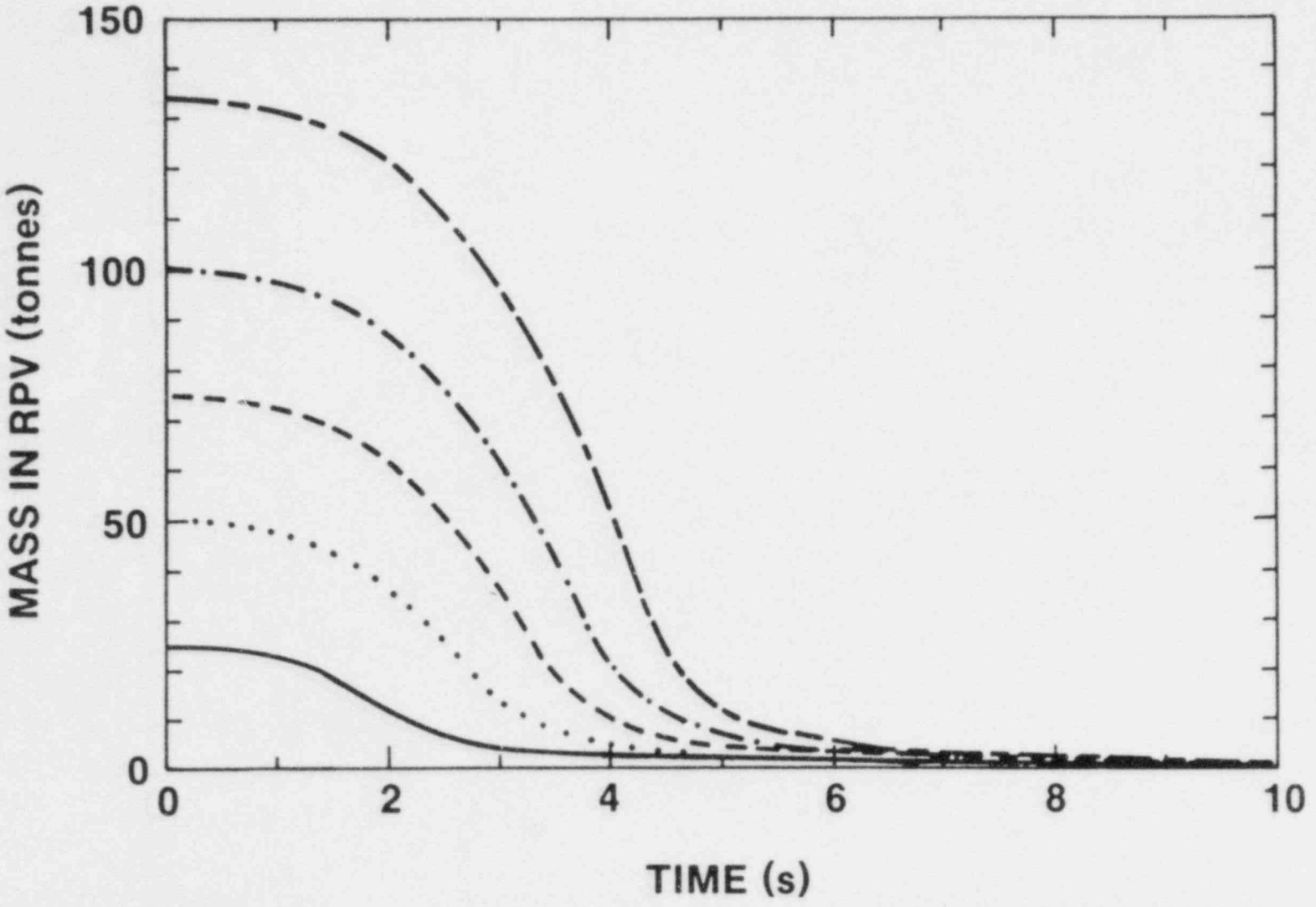

Figure 1. Melt Mass Remaining in Reactor Vessel
Small Break LOCA Accident, P_s=7MPa

holes forming during the discharge process is minimized by the short discharge time assuming a single hole.

3.2 Hole Ablation

Figure 2 shows the hole diameter as function of time and initial mass for the small break LOCA accident. The abrupt change in the ablation rate occurs at the instant of gas blowthrough. Prior to gas blowthrough, the ablation rate is constant; this is because the flat plate heat transfer coefficient is independent of the hole diameter. Following gas blowthrough, the ablation rate rapidly goes to zero; this is because very little molten fuel contacts the hole's surface during the two phase blowdown.

Figure 3 shows that the final size of the hole is insensitive to the pressure that drives fuel from the reactor vessel. This occurs primarily because the higher ablation rate resulting from higher ejection velocities (i.e., higher driving pressure) is offset by shorter ejection times. Notice that the final hole size following gravity drain is slightly larger than the hole size following high pressure ejection of melt.

In a future paper, we will demonstrate that the hole size plays an important role in determining how violently the debris is swept from the cavity.

3.3 Gas Blowthrough

Gas blowthrough occurs before all the melt is ejected from the reactor vessel. Figure 4 shows what fraction of the intial mass remains in the reactor vessel at the instant of gas blowthrough. For a gravity drain, virtually all the mass is drained from the reactor vessel prior to gas blowthrough. For the small break LOCA accident and depending on how much mass is available, 25-50% of the melt remains in the vessel at the instant of gas blowthrough. This is significant.

What happens to the melt remaining in the reactor vessel after gas blowthrough? Is the remaining melt discharged before significant depressurization of the primary system occurs, or does the primary system blowdown first followed by gravity drainage of the remaining melt? We answer this question by examining a small break LOCA accident for the case of 100 tonnes of core debris. Figure 4 shows that about 28 tonne of core debris remains in the reactor vessel at the instant of gas blowthrough (about 3.8 seconds) while Figure 1 shows that only 5 tonnes remains in the vessel at 5.3 seconds. At 5.3 seconds, Figure 5 shows that significant depressurization of the primary system has not occurred before 95% of the melt was ejected from

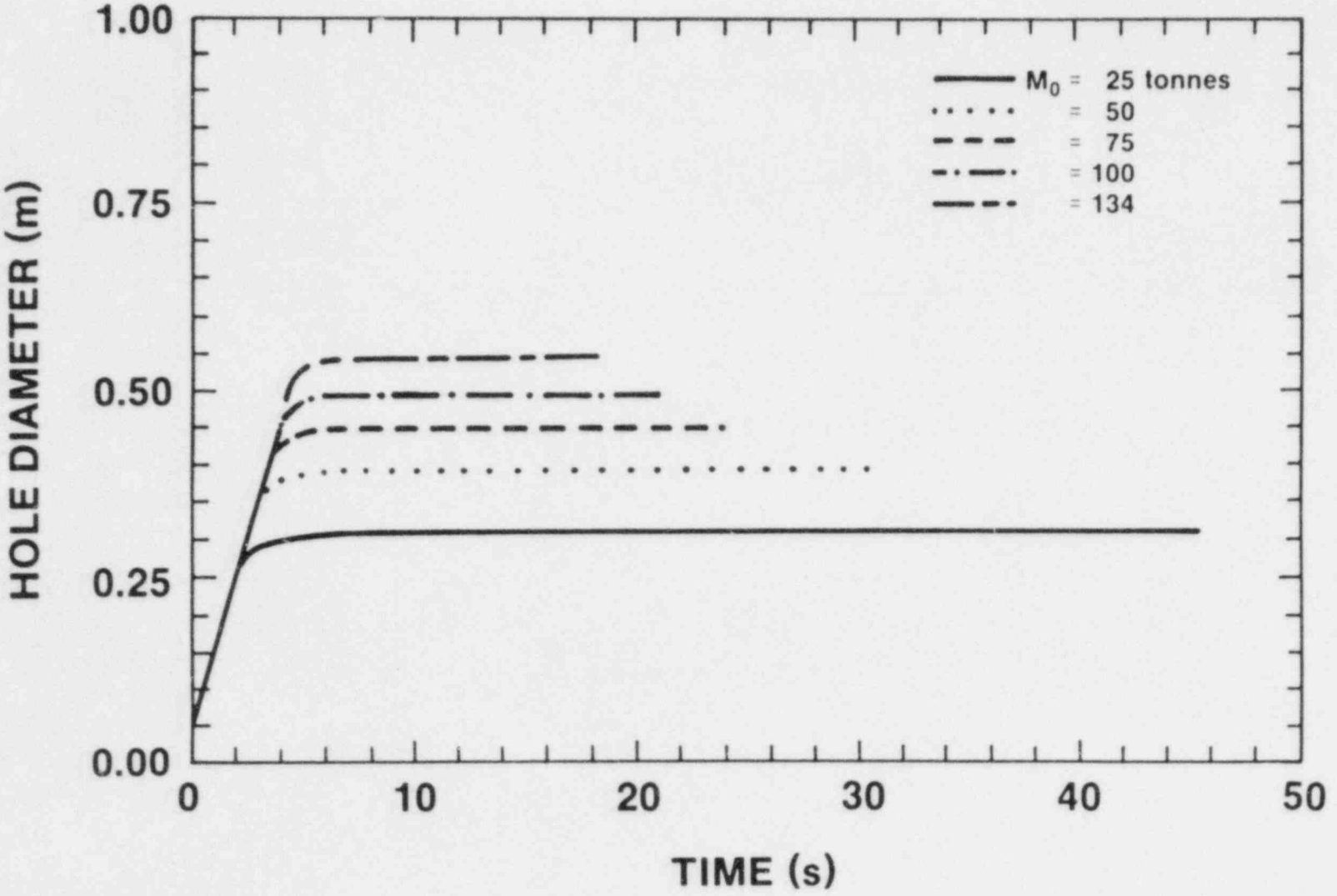

Figure 2. Hole Ablation During Melt Discharge
Small Break LOCA Accident, P_s=7MPa

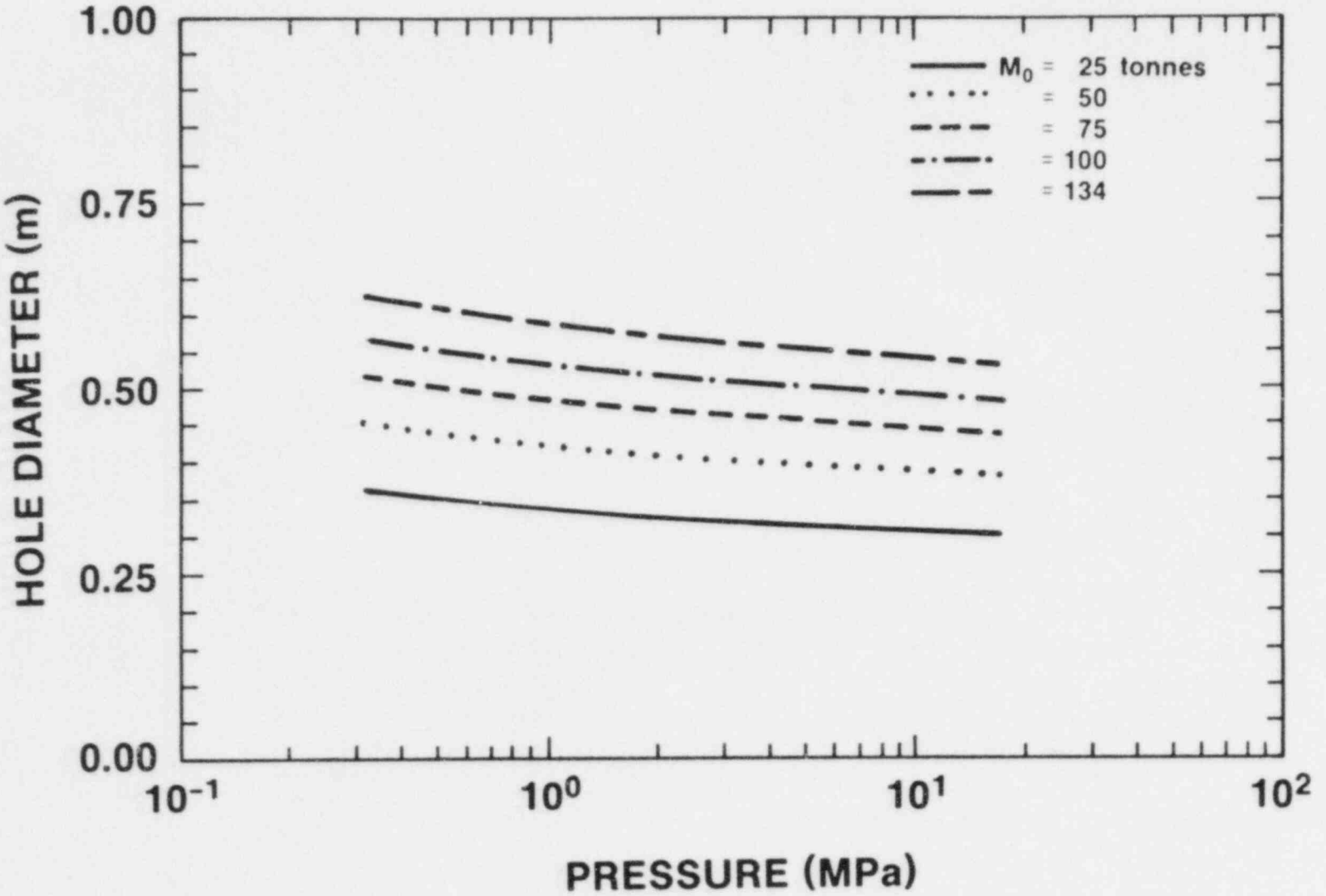

Figure 3. Final Hole Size Following Melt Discharge

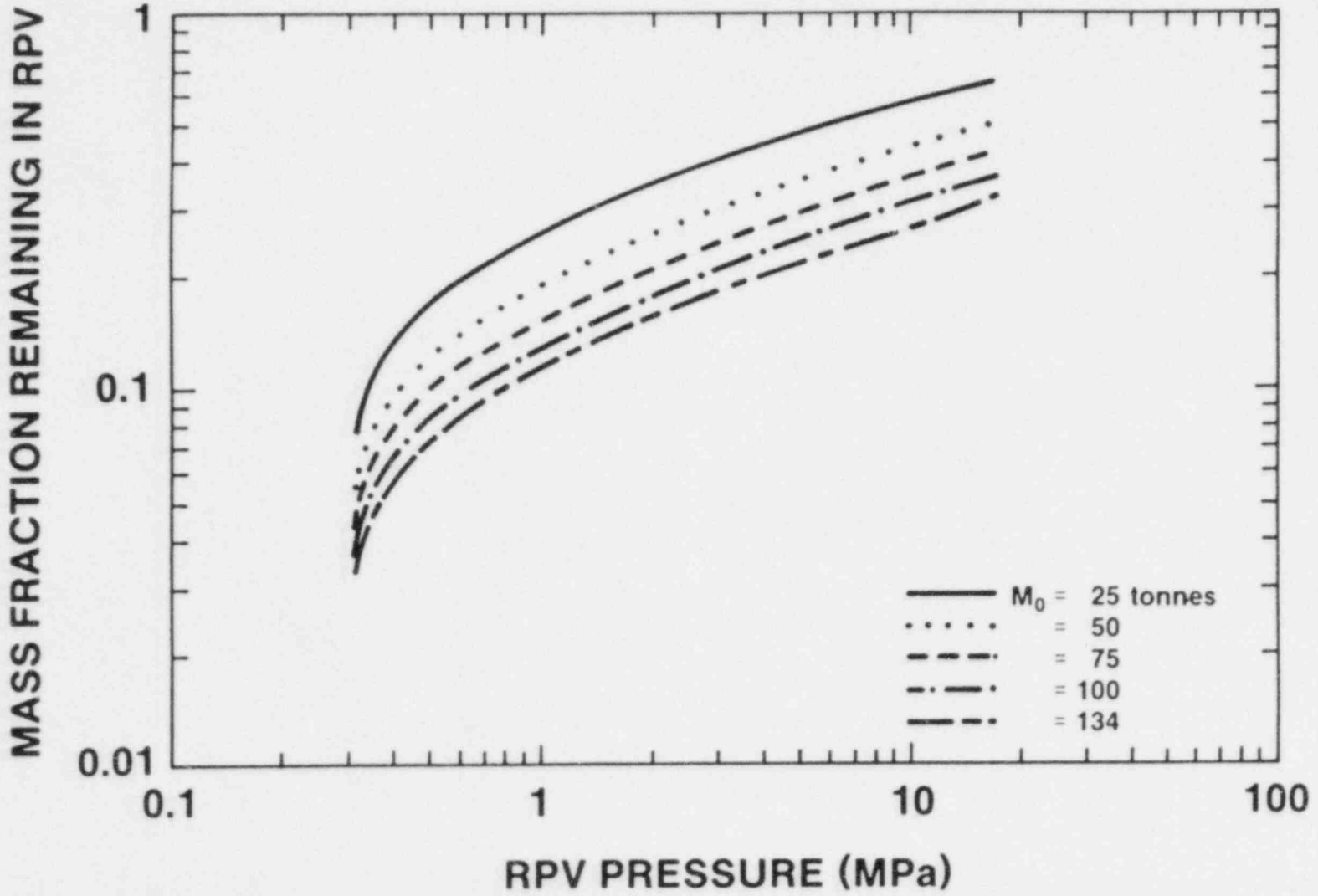

Figure 4. Fraction of the Initial Mass Remaining in the RPV at the Instant of Gas Blowthrough

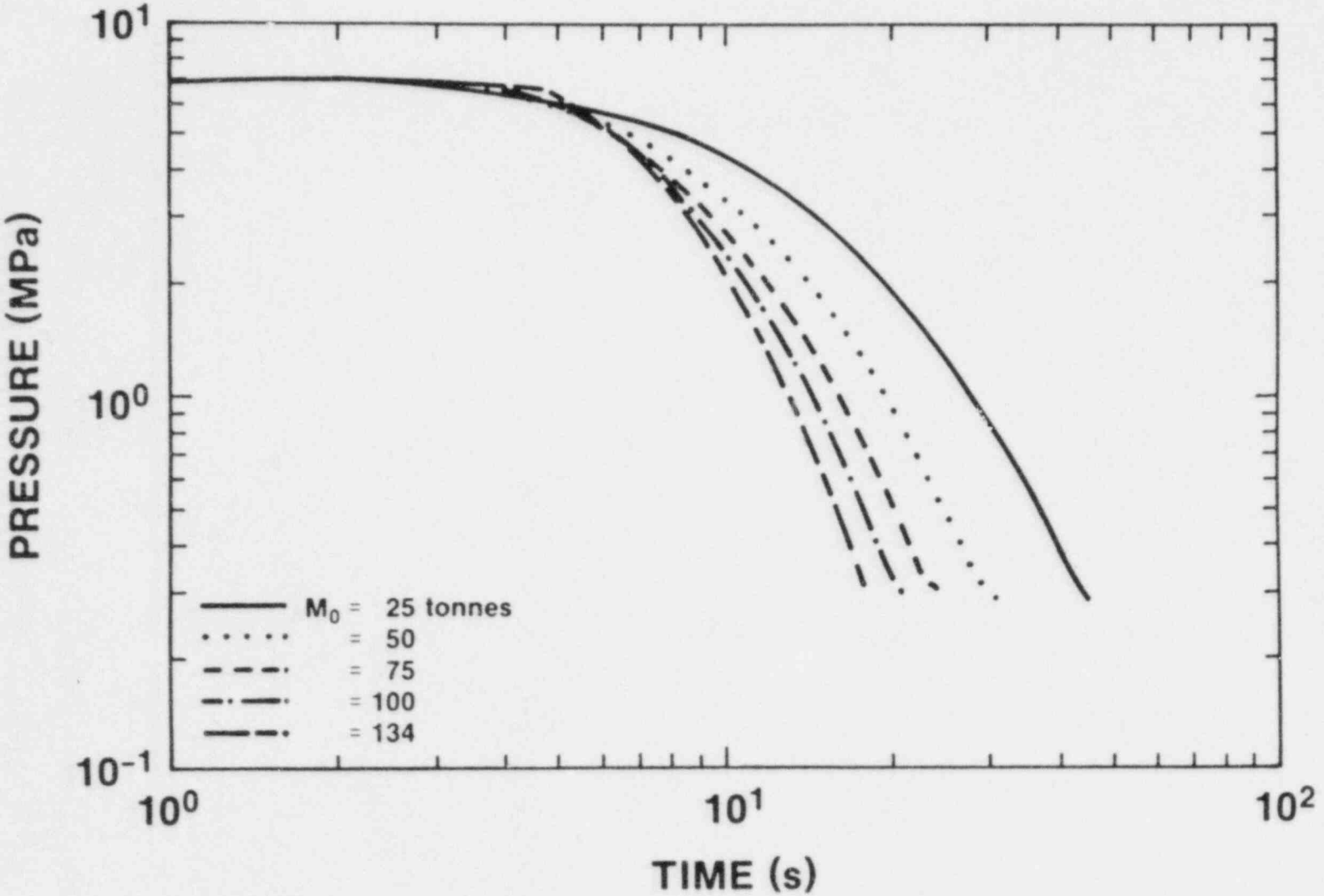

Figure 5. Blowdown of the Primary System
Small Break LOCA Accident, P_s=7MPa

the reactor vessel. We have parametrically investigated the full spectrum of pressures and debris mass, and we find that no more than 25% system depressurization has occurred when only 5% of the mass remains in the reactor vessel. Therefore, we conclude that the melt discharge time is small compared to the blowdown down of the primary system, even when gas blowthrough occurs with significant mass remaining in the reactor vessel.

In SNL's HIPS experiments, gas blowthrough is predicted to occur when approximately 20% of the melt still remains in the melt generator. However, posttest examination of the melt generator confirms our predictions that no melt will remain in the melt generator after blowdown of the pressure vessel is complete.

3.4 Blowdown of the Primary System

Figure 5 shows the pressure of the primary system as a function of time and initial mass for the small break LOCA accident. Blowdown is complete in 20-50 seconds. The range in blowdown times stems from a difference in hole size at the instant of gas blowthrough. Notice that the blowdown time is longer when the debris mass is smaller.

3.5 Pneumatic Atomization

Consider a small break LOCA with 100 tonne of melt in the lower head. Figure 4 shows about 28% of the melt (28 tonnes) remains in the reactor vessel when gas blowthrough begins; this 28 tonnes of melt is pneumatically atomized. The mass median sizes of particles produced by pneumatic atomization (at each instant of time following gas blowthrough) are shown in Figure 6. The calculations are based on a UO_2 surface tension; steel particles will be a factor of 3 larger.

Just after gas blowthrough (3.8 seconds), the particle sizes are large because the gas discharge rate is small (i.e., $\dot{M}_L/\dot{M}_g$ is large). Particle sizes are also large as the blowdown approaches completion (24 seconds). This is because the gas density in the orifice is decreasing (isothermal blowdown of the primary system) and the gas velocity in the orifice is decreasing (flow becomes unchoked).

Notice that the Deysson correlation and the Wigg correlation are in reasonable agreement while Lubanska's correlation can predicts particle sizes that can be an order of magnitude smaller. This reaffirms our caution in extrapolating these correlations to the reactor case.

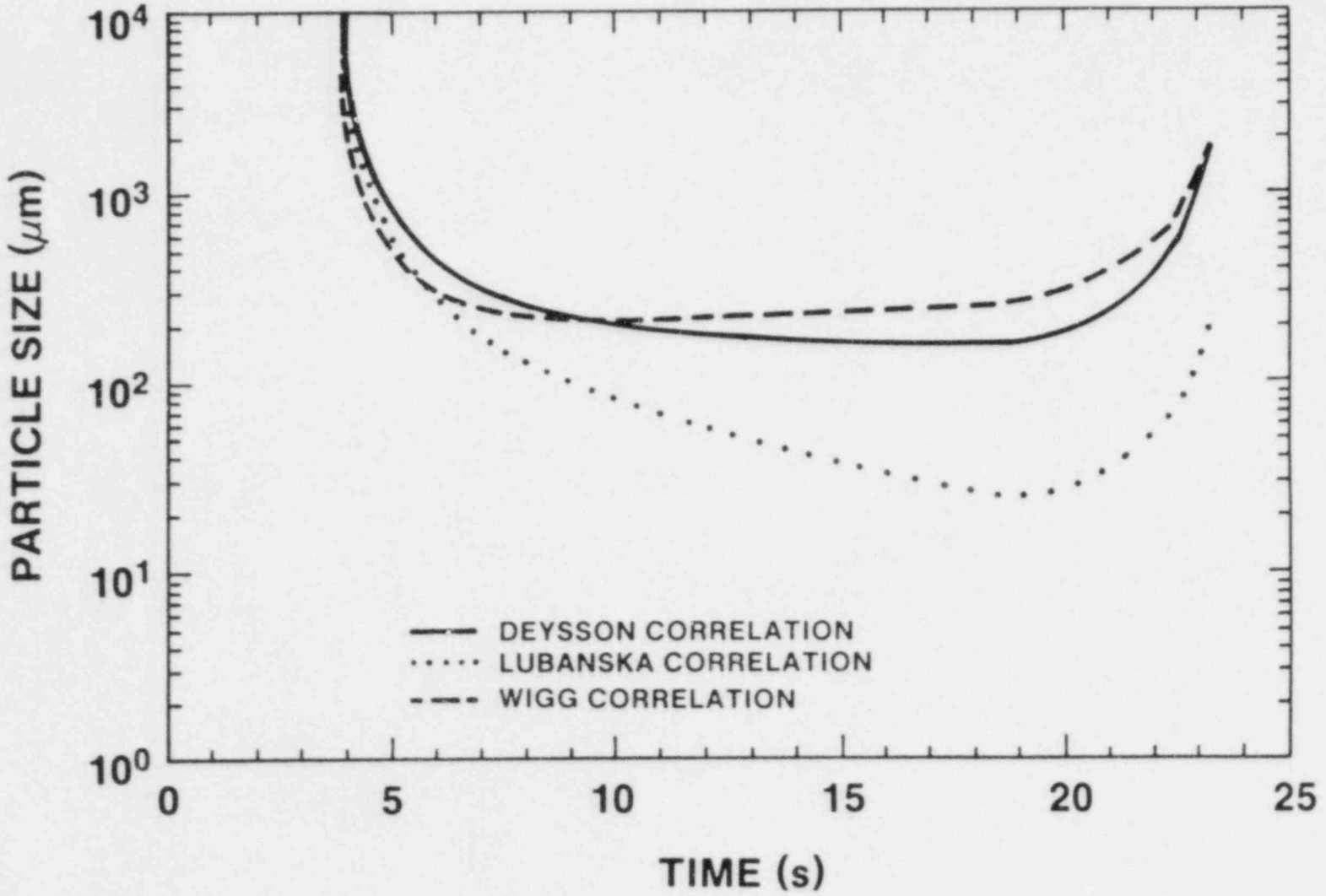

Figure 6. Mass Median Size of Particles Produced by Pneumatic Atomization Small Break LOCA Accident, P_s=7MPa

4. CONCLUSIONS

Melt is rapidly ejected from the reactor vessel when vessel failure occurs while the primary system is still at an elevated pressure. An improved model for hole ablation has been developed. For 100 tonnes of molten debris, the final diameter of the hole is about .5 m, and the final diameter is insensitive to the driving pressure. The ablation rate is constant prior to gas blowthrough. Following gas blowthrough, the ablation rate rapidly goes to zero.

Gas blowthrough is identified as a mechanism that allows steam and hydrogen to escape through the vessel breach before melt ejection is complete. A significant fraction (25-50%) of the initial core debris may still be in the reactor vessel at the instant of gas blowthrough; however, most of this remaining mass is ejected from the reactor vessel before significant depressurization of the primary system occurs.

The melt that is discharged after the onset of gas blowthrough is subject to pneumatic atomization. During much of the blowdown process, the mass median size of particles produced by pneumatic atomization could range from 20μm to 300μm. Prior to gas blowthrough, jet disruption by effervescing hydrogen is expected; however, further research is required to characterized this fragmentation process.

List of Symbols

Symbols

A	Area
C_d	Discharge coefficient
C_p	Specific heat
D	Hole diameter
$\dot{D}$	Ablation rate
d_m	Mass median particle diameter
g	Acceleration due to gravity
H	Instantaneous depth of molten pool inside pressure vessel
H'	Critical pool depth for gas blowthrough
h	Heat transfer coefficient
h_f	Heat of fusion
k	Thermal conductivity
L	Length of hole
M	Mass
$\dot{M}$	Mass flow rate
P	pressure
R	Gas constant
R_g	Gas core radius or gas annulus thickness
T	Temperature
T_m	Melting temperature
V	Velocity

γ Isentropic exponent

ρ Density

σ Surface tension

σ_g Geometric standard deviation in log-normal distribution

μ Viscosity

Subscripts

L Liquid

g Gas

h Hole

c Cavity

f Final

0 Initial

s Surface

w Wall

ps Primary system

mw Molten wall

References

1. Zion Probabilistic Safety Study, Commonwealth Edison Co., Chicago, IL, (Sept. 1981).

2. Indian Point Probabilistic Safety Study, Consolidated Edison Co, Power Authority of the State of New York, (1982).

3. W. Tarbell, J. Brockmann, and M. Pilch, "High-Pressure Melt Streaming (HIPS) Program Plan," SAND82-2477, NUREG/CR-3025, Sandia National Laboratories (Aug. 1984).

4. W. W. Tarbell, M. Pilch, and J. E. Brockmann, "Behavior of Core Debris Ejected From a Pressure Vessel Into Scaled Reactor Cavities," 12th Water Reactor Safety Information Exchange Meeting, Gaithersberg MD, (Oct. 22-26, 1984).

5. J. E. Brockmann, W. W. Tarbell, "Aerosol Source Term in High Pressure Ejection," Nuc. Sci. and Eng., 88, 342-356, (1984).

6. I. Catton, Statements before the Containment Loads Working Group, Argonne National Laboratory, Chicago, Ill., (April 19, 1984).

7. M. F. Young, J. L. Tomkins, and W. J. Camp, "MELPROG Code Development and Methods," International Meeting on Light Water Reactor Severe Accident Evaluation, Cambridge, Mass., Vol. 1, 2.8-1, (Aug. 28 - Sept. 1, 1983).

8. Alan J. Chapman, Heat Transfer, 3rd ed., Macmillan Publishing Co., Inc., (1974).

9. A. J. Suo-Anttila, "Simplified Multicomponent Phase Transition Model," LA-7557-MS, (Jan. 1979).

10. D. F. Gluck, J. P. Gille, E. E. Zukoski, and D. J. Simkin, "Distortion of a Free Surface During Tank Discharge," J. Spacecraft and Rockets, 3(1), 1691-1692, (Nov. 1966).

11. A. Ogunleye, "Removal of Dissolved Hydrogen in Liquid Iron," Second International Congress on Hydrogen in Metals, Paris, France (Jun. 6-11, 1977).

12. J. A. Belk, Vacuum Techniques in Metallurgy, Pergamon Press, 63 (1963).

13. N. A. Warner, "Stream Breakup in Vacuum Degassing," J. Iron and Steel, 44-50 (Jan. 1969).

14. D. A. Powers, "Solubility of Gases in Molten Materials Produced During Reactor Core Meltdowns," SAND83-1796, Sandia National Laboratories (in press).

15. J. Y. Deysson and J. Karian, "Approximate Sizing of Single Fluid and Pneumatic Atomizers," The 1st International Conference on Liquid Atomization and Spray Systems, Tokyo, Japan, 243 (Aug. 27-31, 1978).

16. H. Lubanska, "Correlation of Spray Ring Data for Gas Atomization of Liquid Metals", J. of Metals, 45-48, (Feb. 1980).

17. L. D. Wigg, "Drop-Size Prediction for Twin-Fluid Atomizers," J. Inst. Fuel, 500-505, (Nov. 1964).

18. P. E. Hugo and R. M. German, "Characteristics of Tin Powder Produced by an Annular Gas Atomization Nozzle," Int. J. Powder Metallurgy and Powder Technology, 18(4), 301-311, (1982).

19. James Gretzinger and W. R. Marshall, Jr., "Characteristics of Pneumatic Atomization," AIChE J., 7(2), 312-318, (June 1961).

DISTRIBUTION:

U.S. Government Printing Office
Receiving Branch (Attn: NRC Stock)
8610 Cherry Lane
Laurel, MD 20707
250 Copies for R7

U.S. Nuclear Regulatory Commission (16)
Office of Nuclear Regulatory Research
Washington, DC 20555
Attn: O. E. Bassett
B. S. Burson
R. T. Curtis
C. N. Kelber
J. Larkins
T. Lee (5)
M. Silberberg
R. W. Wright
T. Walker
W. Pasedaq
M. Jankowski
J. Telford

U.S. Nuclear Regulatory Commission (4)
Office of Nuclear Regulatory Regulation
Washington, DC 20555
Attn: L. G. Hulman
P. Easky
J. Rosenthal
J. Mitchell

U.S. Department of Energy (2)
Albuquerque Operations Office
P.O. Box 5400
Albuquerque, NM 87185
Attn: J. R. Roeder, Director
Operational Safety Division
D. K. Nowlin, Director
Special Programs Division
For: C. 3. Quinn
D. Plymale

U.S. Department of Energy
Office of Nuclear Safety Coordination
Washington, DC 20545
Attn: R. W. Barber

Electric Power Research Institute
3412 Hillview Avenue
Palo Alto, CA 94303
Attn: R. Vogel
R. Sehgal

Professor T. Theofanous
Purdue University
School of Engineering
West Lafayette, IN 47907

Fauske & Associates (2)
16W070 West 83rd Street
Burr-Ridge, IL 60521
Attn: Dr. R. Henry
M. Hutcherson

M. L. Corradini
Department of Nuclear Engineering
University of Wisconsin
1500 Johnson Drive
Madison, WI 53706

I. Catton
UCLA
Nuclear Energy Laboratory
405 Hilgard Avenue
Los Angeles, CA 90024

Brookhaven National Laboratory (4)
Department of Nuclear Energy
Building 820
Upton, NY 11973
Attn: R. A. Bari
T. Pratt
G. Greene
T. Ginsberg

Professor R. Seale
Department of Nuclear Engineering
University of Arizona
Tucson, AZ 85721

Oak Ridge National Laboratory (2)
P.O. Box 6
Oak Ridge, TN 37830
Attn: T. Kress
S. Hodge

K. Holtzclaw
General Electric - San Jose
Mail Code 682
175 Kurtner Avenue
San Jose, CA 95125

Argonne National Laboratory
9700 S. Cass Avenue
Argonne, IL 60439
Attn: B. Spencer

Cathy Anderson
Nuclear Safety Oversight Commission
1133 15th St., N.W.
Room 307
Washington, DC 20005

Battelle Columbus Laboratory (3)
505 King Avenue
Columbus, OH 43201
Attn: P. Cybulskis
R. Denning
J. Gieseke

J. E. Antill
Berkeley Nuclear Laboratory
Berkeley GL 139 PB
Gluocestershire
United Kingdom

W. G. Cunliffe
Bldg. 396
British Nuclear Fuels, Ltd.
Springfields Works
Salwick, Preston
Lancs
United Kingdom

Reactor Development Division (4)
UKAEA - Atomic Energy Establishment
Winfrith, Dorchester
Dorset
United Kingdom
Attn: R. G. Tyror, Head
T. Briggs
R. Potter
A. Nichols

Projekt Nucleare Sicherheit (3)
Kerforschungszentrum Karlsruhe
Postfach 3640
75 Karlsruhe
Federal Republic of Germany
Attn: J. P. Hoseman
P. Albrecht
H. H. Rininsland

Mr. G. Petrangeli
Direzione Centrale della Srcurezza
Nucleare e della Protezione Sanitaria (DISP)
Entre Nazionnle Energie Alternative (ENEA)
Vrale Regina Margherita, 125
Casella Postale N. 2358
I-00100 Roma A.D., ITALY

Dr. K. J. Brinkman
Reactor Centrum Nederland
P.O. Box 1
1755 ZG Petten
THE NETHERLANDS

Mr. H. Bairiot, Chief
Department LWR Fuel
Belgonucleaire
Rue de Champde Mars. 25
B-105(Brussels, Belgium

S. Saito
Japan Atomic Energy Research Institute
Takai Research Establishment
Tokai-Mura, Naku-Gun
Ibaraki-ken
Japan

Wang Lu
TVA
400 Commerce, W9C157-CK
Knoxville, TN 37902

M. Fontana
Director, IDCOR Program
Technology for Energy, Inc.
P.O. Box 22996
10770 Dutchtown Road
Knoxville, TN 37922

UKAEA (4)
Safety and Reliability Directorate
Wigshaw Lane
Culcheth
Warrington, WA3 4NE
United Kingdom
Attn: H. J. Teague
I. Cook
A. J. Wickett
P. McBeth

Dr. Fran Reusenbach
Gesellschaft fuer Reaktorsicherheit (GRS mb
Postfach 101650
Glockengasse 2
D-5000 Koeln 1
Federal Republic of Germany

S. J. Niemczyk
Union of Concerned Scientists
1346 Connecticut Avenue. N.W.
S.1101
Washington, DC 200036

M. Jankowski
IAEA
Division of Nuclear Reactor Safety
Wagranerstrasse 5
P.O. Box 100
A/1400 Vienna, Austria

3141	C. M. Ostrander (5)
3151	W. L. Garner (1)
6400	A. W. Snyder
6410	J. W. Hickman
6411	R. D. Gasser
6420	J. V. Walker
6421	T. R. Schmidt
6422	D. A. Powers (5)
6422	J. E. Brockmann (5)
6422	J. E. Gronager
6422	A. L. Ouellette, Jr.
6422	W. W. Tarbell (5)
6422	M. D. Allen
6423	P. S. Pickard
6425	W. J. Camp
6425	D. R. Bradley
6425	M. Pilch (5)
6425	A. Suo Anttila
6425	W. Frid
6427	M. Berman
6430	N. R. Ortiz
6440	D. A. Dahlgren
6442	W. A. Von Riesemann
6449	K. D. Bergeron
6450	J. A. Reuscher
6454	G. L. Cano
7530	T. B. Lane
7537	N. R. Keltner
7537	R. U. Acton
8024	M. A. Pound

NRC FORM 335 (2-84) NRCM 1102, 3201, 3202

U.S. NUCLEAR REGULATORY COMMISSION

BIBLIOGRAPHIC DATA SHEET

SEE INSTRUCTIONS ON THE REVERSE

1 REPORT NUMBER (Assigned by TIDC and Vol. No., if any)
NUREG/CR-4383
SAND85-0012

2 TITLE AND SUBTITLE
HIGH PRESSURE EJECTION OF MELT FROM A REACTOR PRESSURE VESSEL - THE DISCHARGE PHASE

3 LEAVE BLANK

4 DATE REPORT COMPLETED
MONTH: January YEAR: 1985

6 DATE REPORT ISSUED
MONTH: September YEAR: 1985

5 AUTHOR(S)
Marty Pilch
William W. Tarbell

7 PERFORMING ORGANIZATION NAME AND MAILING ADDRESS (Include Zip Code)
Reactor Safety Theoretical Physics Div. 6425
Severe Accident Source Terms Div. 6422
Sandia National Laboratories
Albuquerque, NM 87185

8 PROJECT/TASK/WORK UNIT NUMBER

9 FIN OR GRANT NUMBER
A-1218

10 SPONSORING ORGANIZATION NAME AND MAILING ADDRESS (Include Zip Code)
Division of Accident Evaluation
Office of Nuclear Regulatory Research
U. S. Nuclear Regulatory Commission
Washington, DC 20555

11a TYPE OF REPORT
Final report

b PERIOD COVERED (Inclusive dates)

12 SUPPLEMENTARY NOTES

13 ABSTRACT (200 words or less)

Recent probabilistic risk-assessment studies identified potential accident sequences in which reactor vessel failure occurs while the primary system is at elevated pressure. The phenomenology of the discharge phase is reviewed here. We propose an improved model for hole ablation following vessel failure, and we compare the model with experiment data. Gas blowthrough is identified as a mechanism that allows steam to escape through the vessel breach before melt ejection is complete. Gas blowthrough leads to pneumatic atomization of the remaining melt before significant depressurization of the primary system occurs.

14 DOCUMENT ANALYSIS - a KEYWORDS/DESCRIPTORS
Hole Ablation, Melt Discharge, Atomization, Gas Blowthrough

b IDENTIFIERS/OPEN ENDED TERMS

15 AVAILABILITY STATEMENT
NTIS
GPO Sales

16 SECURITY CLASSIFICATION
(This page) UNCLASSIFIED
(This report) UNCLASSIFIED

17 NUMBER OF PAGES
40

18 PRICE